

## ARTICLE



# Molecular features of primary hepatic undifferentiated carcinoma

Jia-Huei Tsai<sup>1,2</sup>, Yung-Ming Jeng<sup>1,2</sup>, Chia-Hsiang Lee<sup>1</sup> and Jau-Yu Liao<sup>1,2</sup> ✉

© The Author(s), under exclusive licence to United States & Canadian Academy of Pathology 2021

The clinicopathological and molecular characteristics of primary hepatic undifferentiated carcinoma are poorly defined. It is speculated that primary hepatic undifferentiated carcinoma develops in the setting of preceding primary hepatic carcinoma. We investigated 14 primary hepatic undifferentiated carcinomas through targeted next-generation sequencing and immunohistochemistry. A panel of genes commonly mutated in primary liver carcinomas were examined. We found a similar clinical context as primary hepatic carcinoma, including a high prevalence of chronic viral hepatitis (86%), cirrhosis (57%), and elevated alpha-fetoprotein (29%). Tumors had sheet-like and poorly cohesive growth patterns. Rhabdoid cytomorphology was observed in four samples. Notably, the most common genetic mutations in primary hepatic undifferentiated carcinoma were in the promoter of *TERT* ( $n = 8$ , 57%) and *TP53* ( $n = 8$ , 57%), which are common in hepatocellular carcinoma. The mutation rate of *TP53* was elevated compared with hepatocellular carcinoma. No other typical genetic features of intrahepatic cholangiocarcinoma were identified, such as an *IDH1/IDH2* mutation, *FGFR2* fusions, or aberrant BAP1 expression. Furthermore, novel switch/sucrose nonfermenting complex inactivation was found, including *SMARCA4/SMARCA2* ( $n = 1$ ) and *PBRM1* deficiency ( $n = 2$ ). The three tumors demonstrated poorly cohesive histology, including rhabdoid features. High PD-L1 expression (57%) was observed in a majority of the tumors. Primary hepatic undifferentiated carcinoma shares clinical and genetic features with hepatocellular carcinoma but harbors progressive molecular characteristics that may initiate tumor dedifferentiation. High PD-L1 expression in primary hepatic undifferentiated carcinoma may be a useful biomarker for potential immunotherapeutic strategies.

*Modern Pathology* (2022) 35:680–687; <https://doi.org/10.1038/s41379-021-00970-z>

## INTRODUCTION

Primary hepatic undifferentiated carcinoma is a rare hepatic tumor that has been recently added as a diagnostic entity in the fifth edition of the WHO classification of tumors of the digestive system<sup>1</sup>. Primary hepatic undifferentiated carcinoma is defined as a primary liver carcinoma demonstrating no specific cell-lineage differentiation except for a malignant epithelial nature by histology and immunohistochemistry<sup>1</sup>. Until now, no study has investigated this rare tumor except for a few case reports<sup>2–4</sup>. Because primary hepatic undifferentiated carcinoma exhibits no features of hepatocytic or cholangiocytic differentiation, a treatment strategy is uncertain. The lack of readily apparent histopathologic differentiation also hinders a unified and coherent approach to diagnosis and management. Unfortunately, the prognosis of primary hepatic undifferentiated carcinoma appears to be dismal because of its aggressive clinical behavior. Expanding our knowledge of this tumor is vital.

Because primary undifferentiated carcinoma of other organs has been suggested to dedifferentiate from a primary conventional carcinoma<sup>5–7</sup>, we hypothesized that primary hepatic undifferentiated carcinoma may derive from primary hepatic carcinoma (i.e., hepatocellular carcinoma or cholangiocarcinoma). To confirm their biologic relationship, we used a targeted genetic panel encompassing the most commonly mutated genes in

primary hepatic carcinoma to clarify the molecular characteristics of primary hepatic undifferentiated carcinoma. A total of 14 primary hepatic undifferentiated carcinomas were identified at our institute. We examined the biologic relationship, clinicopathological features, and molecular pathogenesis of primary hepatic undifferentiated carcinoma.

## MATERIALS AND METHODS

### Tissue specimens

A total of 5309 cases of primary liver cancer from 2000 to 2019 were found in the archives of the Department of Pathology, National Taiwan University Hospital. We searched for the keywords “undifferentiated carcinoma,” “poorly differentiated carcinoma,” “grade 4 hepatocellular carcinoma,” and “grade 4 cholangiocarcinoma.” The exclusion criteria were biopsy specimens and invasive/metastatic carcinoma from other organs. All histologic slides of the tumors were retrieved for microscopic review. Tumors with histologic evidence of hepatocytic or cholangiocytic differentiation were excluded. Hepatocellular carcinoma is typical for trabecular arrangement of malignant hepatocytes with sinusoidal wrapping endothelium<sup>1</sup>. The tumor cells harbor central-located nuclei, eosinophilic cytoplasm, and prominent nucleoli. In contrast, cholangiocarcinoma is arranged in glandular structures in a densely fibrotic stroma<sup>1</sup>. The nuclei are polarized at the basal part of the cells with variable amounts of mucinous cytoplasm. Immunohistochemical staining for hepatocellular markers, including HepPar-1 and arginase-1, were performed to exclude tumors with positive

<sup>1</sup>Department of Pathology, National Taiwan University Hospital, Taipei, Taiwan. <sup>2</sup>Graduate Institute of Pathology, College of Medicine, National Taiwan University, Taipei, Taiwan. ✉email: 019188@ntuh.gov.tw

expression. We also excluded poorly differentiated carcinoma showing glandular structures or pavement arrangement around the tumor border. A total of 14 primary hepatic undifferentiated carcinomas were identified. All the specimens were resected with the intent of complete tumor resection. Clinical data, including patient demographics, clinical information, imaging features, and clinical outcomes, were obtained from medical records. This study was conducted according to the regulations of the ethics committee of National Taiwan University Hospital. The specimens were anonymous and analyzed in a blinded manner.

### Morphological review

Histologic sections cut at 5  $\mu$ m thickness from 14 primary hepatic undifferentiated carcinomas were stained with hematoxylin and eosin and reviewed by a pathologist to determine their morphologic characteristics, the presence of cirrhosis or cytologic features, and the immunohistochemistry expression pattern. Cirrhosis was present if the nontumor portion was in the F4 stage histologically, according to the Metavir staging system<sup>8</sup>.

### Immunohistochemistry

Tumor tissue (5  $\mu$ m thick) was sectioned from paraffin blocks, and the slides were deparaffinized and rehydrated. The antigens were retrieved by incubating the slides in Epitope Retrieval 2 solution (pH 9.0; Leica Biosystems, Newcastle, UK) or citric acid (pH 6.0) at 100 °C for 10 min. The sections were stained using the Leica Microsystems Bondmax autostainer, according to the manufacturer's protocol. The sections were counterstained with hematoxylin. The clones and dilutions of primary antibodies are summarized in Table 1. Positive staining was defined as the nuclear staining of BAP1, ARID1A, ARID2, PBRM1, SMARCB1, SMARCA4, SMARCA2, and mismatch repair proteins. Loss of expression was defined as the absence of nuclear expression in tumor cells with concurrent positive labeling in stromal cells, lymphocytes, or both. Anti-PD-L1 antibody (clone: SP142) staining was visualized using the OptiView detection kit and the BenchMark ULTRA automated staining platform. The estimated percentage of PD-L1 expression in tumor cells and tumor-associated immune cells was recorded. More than 5% of PD-L1 expression was considered positive for tumor cells and/or tumor-associated immune cells. PD-L1 expression was also graded semi-quantitatively according to the percentage of expression (<5%, 5–10%, 11–50%, and >50%).

### Molecular analysis

Dual-color fluorescence in situ hybridization (FISH) analysis, DNA extraction and targeted next-generation sequencing (NGS) were performed using the methods as previously described<sup>9</sup>. The panel comprised 14 commonly mutated genes in primary liver carcinoma (Supplementary Table 1). All the variants predicted to be pathogenic were validated through Sanger sequencing. The primer sets used for Sanger sequencing are listed in Supplementary Table 2.

### Statistical analysis

Data were analyzed using the SPSS 19.0 software (IBM Corp., Armonk, NY, USA). Comparisons of categorical variables were performed using

Pearson's  $\chi^2$  method or Fisher's exact test. Statistical calculations were performed using Student's *t* test for continuous variables. All statistical results were considered significant if the *P* value was <0.05.

## RESULTS

### Clinical demographics

The clinical features of 14 primary hepatic undifferentiated carcinomas are summarized in Table 2. Table 3 details their clinicopathological characteristics. Almost all of the patients were men ( $n = 13$ , 93%). The mean age was 61 years (range, 41–76 years). A majority of the tumors were in the right lobe ( $n = 9$ , 64%), whereas five tumors (36%) were in the left lobe. The mean diameter of the tumors was 8 cm (range, 3–17 cm). A total of 12 patients (86%) had chronic viral hepatitis, 9 had viral hepatitis B, 1 had viral hepatitis C, and 2 had both viral infections. Cirrhosis of the liver was present in 8 out of 14 (57%) of the primary hepatic undifferentiated carcinomas. Elevation of either CEA and/or CA19-9 was identified in 3 of the carcinomas (21%) and elevation of alpha-fetoprotein was identified in 4 of the carcinomas (29%). Lobectomy was performed in nine patients (64%), atypical hepatectomy was performed in four patients (29%), and segmentectomy was performed in one patient (7%). The anatomic stages were low stage (I–II) in four patients (29%) and high stage (III–IV) in ten patients (71%).

Follow-up information was collected from all patients. The prognosis of the carcinoma was poor. The 5-year survival rate was 57%. Follow-up periods for all survivors ranged from 1 to 208 months with the mean and median survival periods of 60 and 47 months, respectively.

### Histological review

There were two undifferentiated morphologic patterns. One histologic type showed a sheet-like pattern with solid nodules or expansile sheets of malignant cells ( $n = 6$ , 43%) (Fig. 1A). The composing cells were moderate to large undifferentiated cells consisting of hyperchromatic nuclei, varying amounts of cytoplasm, and prominent nucleoli (Fig. 1B). Marked nuclear pleomorphism and anaplasia were frequently seen. Occasional bizarre tumor cells with gigantic polyploid nuclei or multinucleation were observed. High-grade microscopic features were often present,

**Table 1.** Manufacturers, clones, and dilutions of primary antibodies.

Antibody	Manufacturer	Clone	Dilution
BAP1	Santa Cruz, TX, USA	C-4	1:50
ARID1A	Sigma-Aldrich, MO, USA	HPA005456	1:300
ARID2	Bethyl, TX, USA	polyclonal	1:150
PBRM1	Bethyl	polyclonal	1:500
SMARCB1	Sigma-Aldrich	2C2	1:50
SMARCA4	Santa Cruz, TX, USA	H-88	1:50
SMARCA2	BD, CA, USA	24/BRM	1:50
PDL1	Ventana, AZ, USA	SP142	1:100
PMS2	Dako Cytomation, CA, USA	EP51	1:50
MLH1	Dako Cytomation	ES05	1:100
MSH6	Dako Cytomation	EP49	1:200
MSH2	Dako Cytomation	FE11	1:200

**Table 2.** Clinical features of primary hepatic undifferentiated carcinoma.

Clinical features	Number, $n = 14$ (%)
Sex (male)	13 (93%)
Age (mean, range)	61 (41–76)
Tumor location	
Right lobe	9 (64%)
Left lobe	5 (36%)
Tumor size (cm, range)	8 (3–17)
Viral hepatitis	12 (86%)
Cirrhosis	8 (57%)
Elevation of CEA or CA19-9 ( $n = 6$ )	3 (21%)
Elevation of AFP ( $n = 13$ )	4 (29%)
Operation	
Lobectomy	9 (64%)
Atypical hepatectomy	4 (29%)
Segmentectomy	1 (7%)
TNM anatomic stage	
I–II	4 (29%)
III–IV	10 (71%)

**Table 3.** Clinical characteristics of primary hepatic undifferentiated carcinoma.

No	Sex	Age	Viral hepatitis	CEA (ng/ml)	CA199 (U/ml)	AFP (ng/ml)	Cirrhosis	Previous history	Tumor location	Tumor size (cm)
1	M	61	HBV			<20	y	HCC	R	2.5
2	M	68	HCV	0.6		24	y		R	7
3	F	70	nil	0.52			n		L	5.5
4	M	48	HBV	4.61	65.7	51.66	y		R	10
5	M	59	HBV	3.85		9	y		R	11
6	M	46	HBV			7687	y	HCC	L	8
7	M	70	HBV			1.99	n		L	9
8	M	54	both	0.32	8.8	88.75	n	HCC	R	3
9	M	65	HBV	5.79	115	5.32	y		R	11
10	M	72	nil				y		R	5.8
11	M	69	both			9127	y		L	4.5
12	M	52	HBV	1.93	17.38	2.43	n		R	17
13	M	41	HBV			7.29	n		R	9
14	M	76	HBV			2.35	n		L	7
No	Image findings							Operation	Stage	Outcome
1	CT: A perfusion defect lesion.							Atypical lobectomy	II	DOD
2	CT: Necrotic tumor or abscess. MRT: Heterogeneous enhanced tumor with necrosis and hemorrhage.							Atypical hepatectomy	III	DOD
3	CT: A hypovascular tumor.							Atypical hepatectomy	IV	DOD
4	CT: A hypovascular tumor, abscess, or necrotic tumor. MRI: low signal on T1WI, mild high signal on T2WI, with mild marginal enhancement through delayed phase.							Atypical lobectomy	IV	DOD
5	na.							Lobectomy	III	DOD
6	CT: A well-defined hypervascular lesion. MRI: global enhancement in arterial phase, and washout in venous phase.							Atypical hepatectomy	II	DOD
7	CT: A large lobulated hypodense tumor with mild dilated intrahepatic duct.							Lobectomy	III	DOD
8	CT: 3.8 cm hepatic tumor with peripheral enhancement on both early arterial phase and venous phases.							Segmentectomy	I	LF
9	CT: An abdominal mass, with left portal vein thrombi.							Atypical hepatectomy	III	DOD
10	CT: An ill-defined hypodense lesion. MRI: polypoid enhanced nodules.							Extended right lobectomy	IV	DOD
11	CT: A hypervascular tumor with portal venous washout.							Lobectomy	II	AWD
12	CT: A mass lesion with washout in venous phase.							Lobectomy	IV	AWD
13	CT: A lobular mass with heterogeneous enhancement. MRI: mixed low and high signal on T1WI, heterogeneous high signal on T2WI, and with heterogeneous enhancement.							Extended right lobectomy	III	AWOD
14	MRI: hypointensity on T1-weighted images, slight hyperintensity on T2-weighted images, and global enhancement on early arterial phase, rapid washout on delayed enhanced images.							Left lateral lobectomy	III	DOD

AWD alive with disease, AWOD alive without disease, CT computed tomography, DOD death of disease, HCC hepatocellular carcinoma, LF lost in follow-up, MRI magnetic resonance imaging, na not available.

such as brisk mitoses, geographic necrosis, and frequent vascular permeation. Extensive necrosis can result in a tumor with a peritheliomatous growth pattern. Other common features included extensive tumor infarct, stromal fibrosis, and hemorrhage.

The other undifferentiated histologic type demonstrated a poorly cohesive pattern with predominant poorly cohesive to discohesive tumor growth ( $n = 8$ , 57%) (Fig. 1C). The malignant cells were medium to large, harboring round to oval nuclei, prominent central nucleoli, and vesicular chromatin (Fig. 1D). Strikingly, four of the eight tumors displayed rhabdoid morphology characterized by eccentric nuclei and abundant eosinophilic cytoplasm (Fig. 1E).

Seven primary hepatic undifferentiated carcinomas showed rich inflammatory infiltrate in the tumor and associated stroma

(Fig. 1F). Variable degrees of inflammatory cell infiltrate were found in the other samples.

#### Molecular alterations in primary hepatic undifferentiated carcinoma

Several molecular derangements were found through targeted NGS and immunohistochemistry in primary hepatic undifferentiated carcinomas; they are illustrated schematically in Fig. 2. Targeted NGS was successfully performed in all tumors. The mean target sequencing coverage was  $1539 \pm 830$  unique reads for the target interval from 111 to 127. The most common genetic mutations in primary hepatic undifferentiated carcinoma were in the promoter of *TERT* (*pTERT*) ( $n = 8$ , 57%) and *TP53* ( $n = 8$ , 57%). The other pathogenic mutations were also identified in *KRAS* ( $n = 2$ ) and *GNAS* ( $n = 1$ ). Five primary hepatic undifferentiated



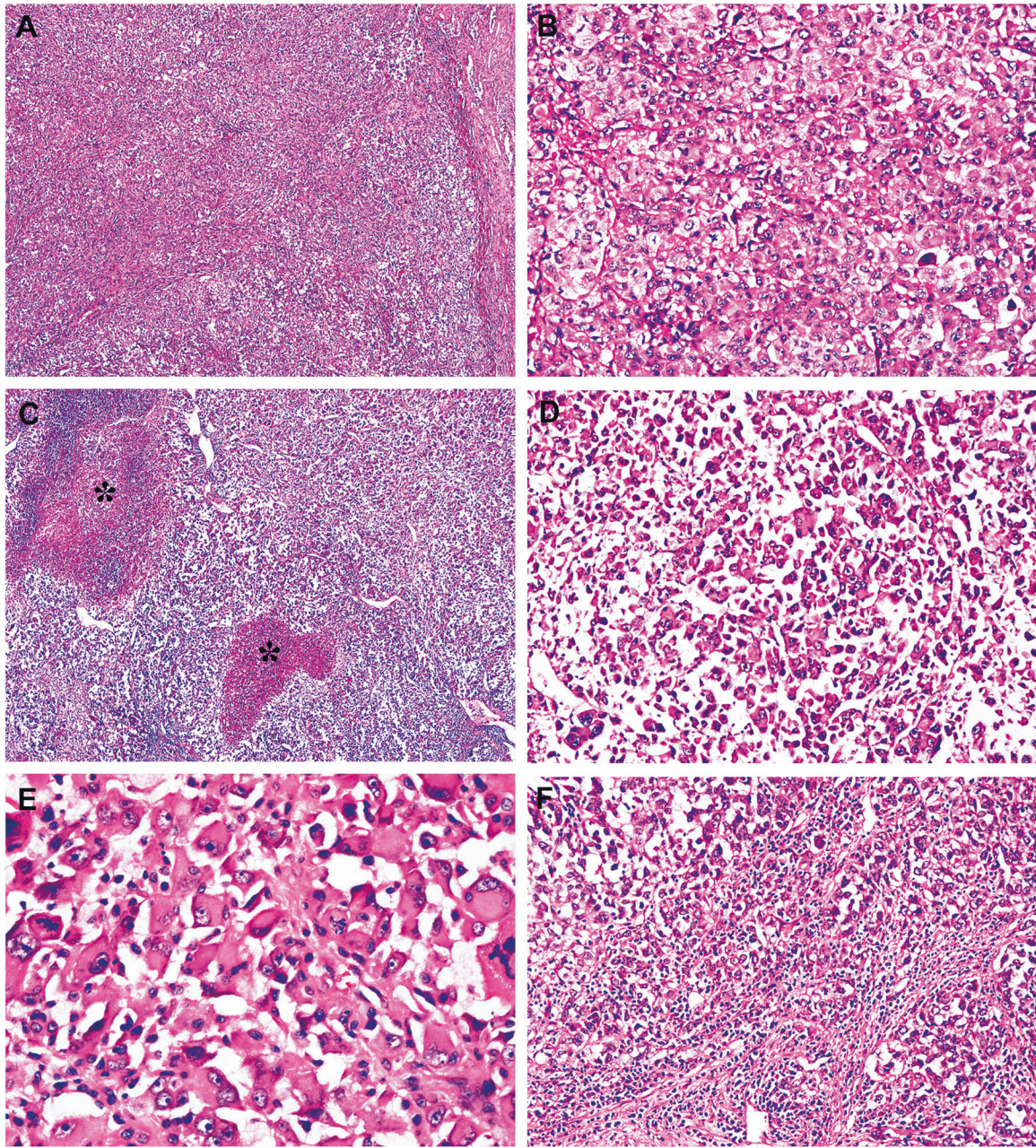


**Fig. 1 Pathological features of primary hepatic undifferentiated carcinoma.** **A, B** A predominant sheet-like growth pattern is characterized by expansive sheets of undifferentiated tumor cells. **C, D** A predominant poorly cohesive growth pattern is composed of poorly cohesive to discohesive tumor cells. The asterisk denotes geographic necrosis. **E** Rhabdoid cytomorphology demonstrated enlarged nuclei, prominent nucleoli, vesicular chromatin, and typical abundant eccentric eosinophilic cytoplasm. **F** Seven samples demonstrated rich lymphoid infiltrate in tumor and tumor-associated stroma.

carcinomas had concurrent *pTERT* and *TP53* mutations. Mutations in *CTNNB1*, *IDH1*, *IDH2*, *BRAF*, *AKT1*, *PIK3CA*, *ERBB2*, *ERBB3*, and *EGFR* were not identified. All the pathogenic variants were validated through Sanger sequencing. The variants and details of the mutated genes are summarized in Supplementary Table 3. Somatic variants of unknown significance are listed in Supplementary Table 4.

Microscopically, frequent loss of expression of the switch/sucrose nonfermenting (SWI/SNF) complexes was detected in primary hepatic undifferentiated carcinomas ( $n = 6$ , 43%). Expression of *ARID1A* and *PBRM1* was deficient in three and two samples, respectively (Fig. 3A, B). One tumor with deficient *SMARCA4* expression also showed a loss of *SMARCA2* expression

(Fig. 3C). Loss of expression of *ARID1A*, *SMARCA4/SMARCA2*, and *PBRM1* were mutually exclusive. All the three samples with a loss of *SMARCA4/SMARCA2* and *PBRM1* showed a poorly cohesive histologic pattern and two of them displayed a mostly rhabdoid morphology. Two of the *ARID1A*-deficient tumors showed a sheet-like growth pattern and one demonstrated a poorly cohesive morphology. Expression of *BAP1*, *ARID2*, *SMARCB1*, and mismatch repair proteins (*PMS2*, *MLH1*, *MSH6*, and *MSH2*) was preserved in all tumors. *FGFR2* fusions were not observed in FISH analysis.

#### PD-L1 expression

Notably, a majority of the primary hepatic undifferentiated carcinomas ( $n = 11$ , 79%) exhibited PD-L1 expression in the



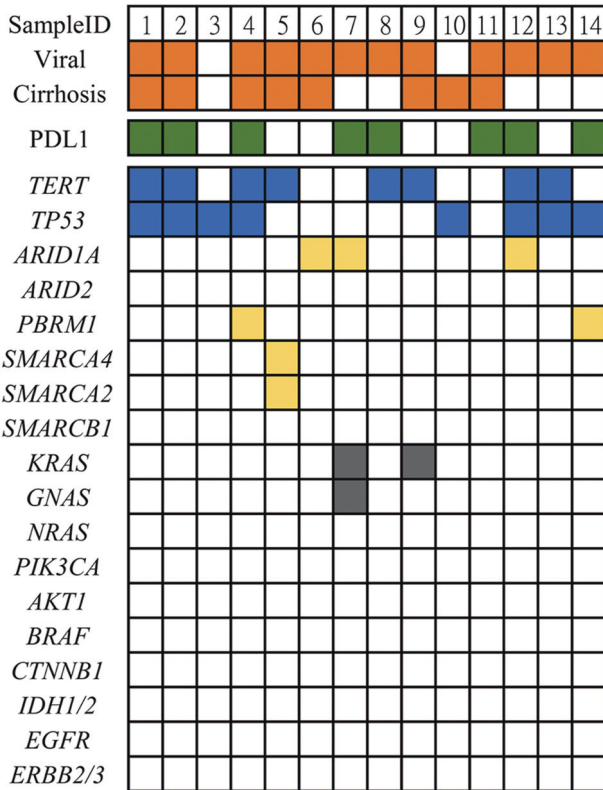


**Fig. 2 Schematic illustration of genetic alterations in primary hepatic undifferentiated carcinoma.** The top panel shows presence or absence of relevant risk factors (viral hepatitis and cirrhosis). The middle panel shows tumors with positive PD-L1 expression. The lower panel shows genetic alterations in primary hepatic undifferentiated carcinoma. The most common mutations were in pTERT and TP53. Other frequent alterations were in the chromatin regulators (loss of expression for ARID1A, PBRM1, SMARCA4 and SMARCA2).

immune cells. The expression was 5–10% in 0 (0%), 10–50% in 9 (64%), and >50% in 2 (14%). A total of eight primary hepatic undifferentiated carcinomas (57%) demonstrated high PD-L1 expression in tumor cells (Fig. 3D). Seven of them showed a >50% tumor expression rate, one displayed a 10–50% rate, and none demonstrated a 5–10% rate. Strikingly, expression in tumor cells was strongly associated with the presence of rich inflammatory infiltrate in the tumor and tumor-associated stroma ( $P = 0.005$ ).

**DISCUSSION**

Primary hepatic undifferentiated carcinoma is a rare hepatic malignancy. Until now, only a few cases have been described, but case numbers were too few to characterize this neoplasm<sup>2–4</sup>. At our institute, we identified 14 primary hepatic undifferentiated carcinomas from the past 10 years, and the incidence of primary hepatic undifferentiated carcinomas in primary hepatic carcinoma was ~0.26%. Although primary hepatic undifferentiated carcinoma has been recently proposed as a diagnostic entity by the fifth edition of the WHO classification of tumors of the digestive system<sup>1</sup>, the clinicopathological and molecular phenotypes remain unclear. To our knowledge, this study is the first case series with in-depth histopathological and molecular analyses. We explored targeted NGS and immunohistochemistry in primary hepatic undifferentiated carcinoma and identified high mutation rates of the *pTERT* and *TP53* genes and the inactivation of SWI/SNF complexes.

Notably, molecular alterations of *pTERT/TP53* were genetically characteristic in hepatocellular carcinoma<sup>10–13</sup>. In particular, the occurrence of the *pTERT* mutation in hepatocellular carcinoma was reported to be ~60%<sup>10–13</sup>, which is similar to the *pTERT* mutation rate of primary hepatic undifferentiated carcinoma in this study (57%). In contrast, no other typical genetic features of cholangiocarcinoma were identified (such as *IDH1/IDH2* mutation, *FGFR2* fusions, or aberrant BAP1 expression)<sup>14–16</sup>. In more, we found similar clinical context between primary hepatic undifferentiated carcinoma and hepatocellular carcinoma, such as a high prevalence of chronic liver disease, mainly with viral hepatitis, cirrhosis, and the presence of elevated alpha-fetoprotein in some of the patients. Because of the shared clinical and molecular features, it is quite conceivable that primary hepatic undifferentiated carcinoma transforms from a previous hepatocellular carcinoma.

Notably, we detected an elevated frequency of *TP53* mutation and SWI/SNF complex inactivation in primary hepatic undifferentiated carcinoma compared with hepatocellular carcinoma. Genome profiling of hepatocellular carcinoma has revealed a *TP53* mutation rate of approximately 30%<sup>10–13</sup>. The most commonly mutated gene encoding subunits of the SWI/SNF complex in hepatocellular carcinoma were *ARID1A* and *ARID2*, with an occurrence rate of 15% and 5%, respectively<sup>10–13,17,18</sup>. Mutations in *PBRM1* and *SMARCA4* were rare in hepatocellular carcinoma; the average mutation frequency was 2%<sup>17</sup>. Overall, alterations in the *TP53* gene and SWI/SNF complex in hepatocellular carcinoma were 30% and 20–25%, respectively. In our study, *TP53* and the SWI/SNF complexes was aberrant in approximately 57% and 43% of primary hepatic undifferentiated carcinomas, respectively, which is roughly two times higher than the mutation rate of hepatocellular carcinoma. The increase in *TP53* and the presence of novel SWI/SNF complexes aberrations may play an important role in tumor progression and the undifferentiated histology.

Morphologic phenotypes of hepatocellular carcinoma have been correlated with distinct genetic defects<sup>19,20</sup>. For instance, *CTNNB1*-mutated hepatocellular carcinoma mainly exhibits a well-differentiated histology, whereas *TP53*-mutated tumors demonstrate an often poorly differentiated and compact morphology. Furthermore, hepatocellular carcinoma with *TP53* mutation is specifically associated with amplified nuclear ploidy and poor differentiation<sup>21</sup>. Therefore, undifferentiated carcinoma may present one end of the histologic spectrum in *TP53*-mutated hepatocellular carcinoma.

Similarly, SWI/SNF complexes have been identified to be defective in several undifferentiated malignancies of other organs<sup>5,6,18,22–24</sup>. Most rhabdoid tumors have a pathogenic mutation in *SMARCB1*. An inactivating mutation of *SMARCA4* has often been found in small-cell carcinoma of the ovary, hypercalcemic type<sup>18,22,23</sup>. Both of these tumors are undifferentiated malignancies and display highly aggressive clinical behavior. Rhabdoid morphology with eccentric nuclei, prominent nucleoli, and eosinophilic cytoplasm was observed in the two neoplasms. The loss of *SMARCA4/SMARCA2* has also been recognized in undifferentiated carcinoma of the esophagus and lung<sup>6,7</sup>. In endometrial undifferentiated carcinoma, *SMARCB1* or *SMARCA4* expression was absent in the undifferentiated component but preserved in the low-grade component, suggesting that *SMARCB1* or *SMARCA4* deficiency is highly correlated with tumor dedifferentiation<sup>5</sup>. Consistent with these findings, we detected *SMARCA4/SMARCA2* deficiency in one sample, which displayed a typical rhabdoid cytomorphology. Notably, two other samples with loss of *PBRM1* expression were identified. Of them, one showed a rhabdoid histology and the other exhibited extensive cell discohesion. *PBRM1* loss has been reported in the rhabdoid variant of renal cell carcinoma and in undifferentiated carcinoma of the gallbladder<sup>25–27</sup>. The above findings support that inactivation of SWI/SNF complexes contributes to tumor dedifferentiation.

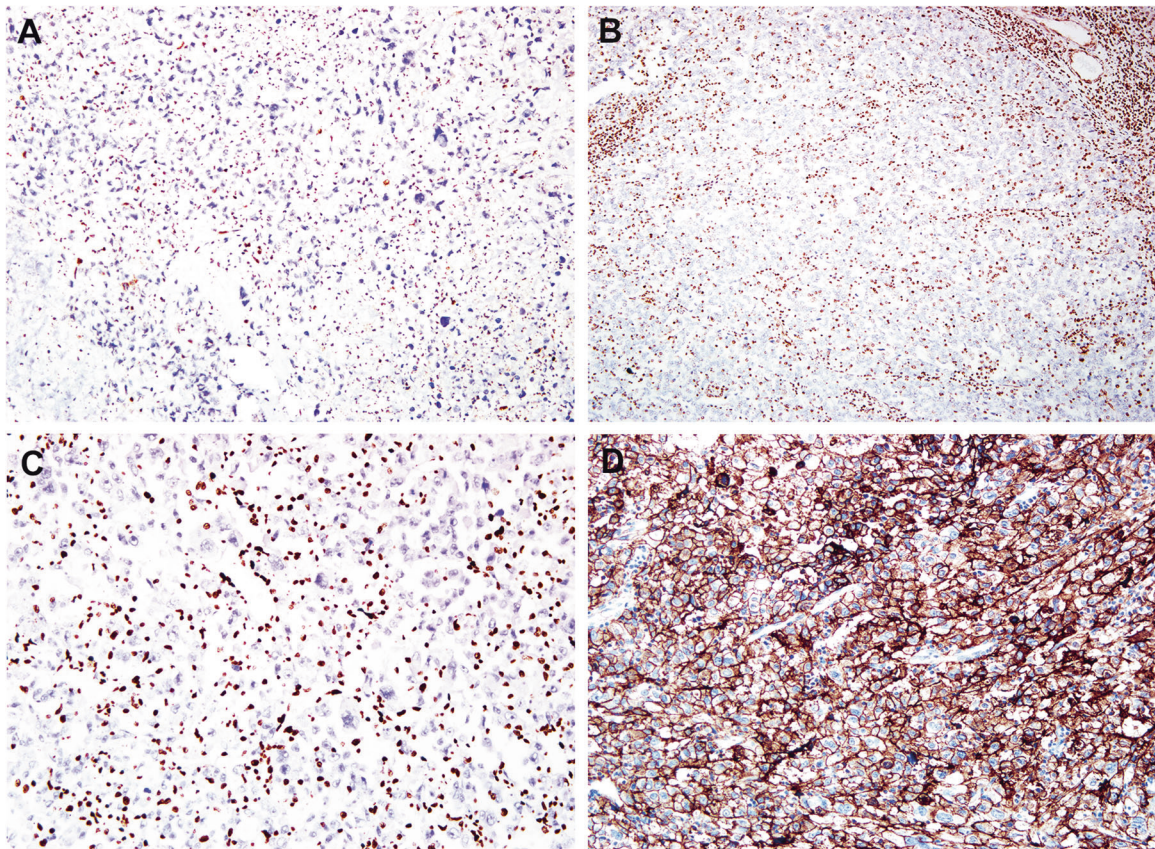


**Fig. 3 Immunohistochemical expression of primary hepatic undifferentiated carcinoma.** Frequent loss expression for SWI/SNF complexes is observed. There is loss of expression for ARID1A (A), PBRM1 (B), and SMARCA4 (C), respectively. (D) shows strong PD-L1 expression in tumor cells and associated immune cells.

SWI/SNF chromatin-remodeling complexes are essential in the regulation of a variety of cellular processes, including cell cycle control, cell differentiation, and DNA repair<sup>22–24</sup>. The complexes consist of 12–15 macromolecular assemblies and exert their regulatory function through adenosine triphosphate-dependent nucleosome remodeling. Although the tumorigenesis mechanism of SWI/SNF complexes remains elusive, it is well recognized that defective SWI/SNF complexes predisposes cells to carcinogenesis<sup>22–24</sup>. In addition, *SMARCA4* and *SMARCA2* were found to be involved in the regulation of cell-adhesion molecules and cytoskeleton structures<sup>24</sup>. Similarly, *PBRM1* plays a role in controlling the expression of cell-adhesion proteins<sup>28,29</sup>. The close association of poor cohesive histology and rhabdoid morphology with SWI/SNF deficiency in the present study implies that tumor dedifferentiation may result from the aberrant functioning of SWI/SNF complexes, especially *SMARCA4*, *SMARCA2*, and *PBRM1*. In this regard, SWI/SNF complexes may not only promote tumor development but also be involved in stepwise malignant progression. Undifferentiated histology appears to predict an unfavorable prognosis for an aggressive clinical course in primary hepatic undifferentiated carcinoma.

One of the most significant findings of this study was the identification of a high expression of PD-L1 in more than half of the cases of primary hepatic undifferentiated carcinoma reviewed. Because PD-L1 expression detected by SP142 antibody was reported to have a lower labeling score than other commonly used clones, such as 22C3, 28-8, and E1L3N antibodies<sup>30</sup>, the expression of PD-L1 in primary hepatic undifferentiated carcinoma could be higher if other immunohistochemical assays were performed. PD-L1 expression was shown to be a potential biomarker of response to immunotherapy with immune

checkpoint inhibitors<sup>31</sup>. As a result, immunotherapy may benefit patients with tumors with high PD-L1 expression. Furthermore, several SWI/SNF targeted treatments have emerged as therapeutic options in cancers with aberrant SWI/SNF function<sup>22</sup>. Whether primary hepatic undifferentiated carcinoma is vulnerable to immunotherapy or SWI/SNF targeted therapy is unknown; further clinical management studies are mandatory.

Although *CTNNB1* is one of the core driver genes in hepatocellular carcinoma<sup>10–13</sup>, we did not find *CTNNB1* mutation in primary hepatic undifferentiated carcinoma. Because *CTNNB1* mutation is correlated with well-differentiated histology and nonproliferative phenotype in hepatocellular carcinoma<sup>19,20,32</sup>, it was not surprising to detect wild-type *CTNNB1* in all the primary hepatic undifferentiated carcinomas, which were not only undifferentiated but highly proliferative. Lack of *CTNNB1* mutation also demonstrates a morpho-molecular correlation in hepatocellular carcinoma. Because this study was a retrospective analysis, the observations between morphologic features and genetic changes (such as SWI/SNF alterations and lack of *CTNNB1* mutation) may not be necessarily causative. Morpho-molecular correlation in hepatocellular carcinoma were more well-validated in the other entities, such as macrotrabecular-massive hepatocellular carcinoma and fibrolamellar hepatocellular carcinoma<sup>33–35</sup>. Macrotrabecular-massive hepatocellular carcinoma is a distinct morphologic subtype of hepatocellular carcinoma that exhibits a predominant macrotrabecular architecture and specific molecular features<sup>1</sup>. The neoplasm is characterized by *TP53* mutation, *FGF19* amplification, and high expression of neoangiogenesis-related genes<sup>20,33,34</sup>. Fibrolamellar hepatocellular carcinoma harbors a signature genetic feature of *DNAJB1-PRKACA* fusion and histologically, displays large polygonal cells with vesicular nuclei, large



nucleoli, and abundant eosinophilic cytoplasm<sup>1,35</sup>. Stromal lamellar fibrosis is also characteristic. The above examples demonstrate a high degree of histological heterogeneity and genotype-phenotype correlation in hepatocellular carcinoma.

The limitations of this study include a small sample size and a targeted genetic panel but not extensive genome profiling. Because primary hepatic undifferentiated carcinoma is a rare hepatic neoplasm, this study expanded our knowledge about the histologic and molecular features of this tumor. The targeted genetic panel used in this study included the most commonly mutated genes in primary hepatic carcinoma. This study compared the similarity and differences between primary hepatic carcinoma and primary hepatic undifferentiated carcinoma. We identified a similar genetic signature in the two entities, supporting a biologic linkage. Furthermore, the identification of an elevated *TP53* mutation rate and the loss of SWI/SNF complexes in primary hepatic undifferentiated carcinoma also support stepwise progressive molecular pathogenesis. However, more extensive studies are needed to explore the detailed genetic features of primary hepatic undifferentiated carcinoma.

In summary, primary hepatic undifferentiated carcinoma shares genetic similarities with primary hepatic carcinoma and is characterized by progressive molecular alteration including elevated frequency of *TP53* mutation and SWI/SNF deficiency. We frequently encountered high PD-L1 expression by tumor cells. Because primary hepatic undifferentiated carcinoma harbored no specific histologic differentiation, clinical management should be directed by its genetic features and approached with urgency. Potential therapeutic strategies, such as the application of immune checkpoint inhibitors or SWI/SNF targeted molecules, warrant further investigation.

#### DATA AVAILABILITY

The data that support the findings of this study are available from the corresponding author upon reasonable request.

#### REFERENCES

- WHO Classification of Tumours Editorial Board. Digestive system tumours. Lyon (France): International Agency for Research on Cancer; p262, 2019. (WHO classification of tumours series, 5th ed. vol. 1).
- Maeda, T. et al. Undifferentiated carcinoma of the liver: a case report with immunohistochemical analysis. *Surg. Case Rep.* **3**, 12 (2017).
- Ochi, T. et al. Undifferentiated carcinoma of the liver in a 3-year-old girl treated by neoadjuvant chemotherapy and complete resection. *Int. J. Surg. Case Rep.* **78**, 67–70 (2021).
- Ogasawara, N. et al. Undifferentiated carcinoma of the liver demonstrated by contrast-enhanced ultrasonography. *Clin. J. Gastroenterol.* **13**, 1225–1232 (2020).
- Karnezis, A. N. et al. Loss of switch/sucrose non-fermenting complex protein expression is associated with dedifferentiation in endometrial carcinomas. *Mod. Pathol.* **29**, 302–314 (2016).
- Horton, R. K. et al. SMARCA4/SMARCA2-deficient carcinoma of the esophagus and gastroesophageal junction. *Am. J. Surg. Pathol.* **45**, 414–420 (2021).
- Rekhtman, N. et al. SMARCA4-deficient thoracic sarcomatoid tumors represent primarily smoking-related undifferentiated carcinomas rather than primary thoracic sarcomas. *J. Thorac. Oncol.* **15**, 231–247 (2020).
- Bedossa, P. & Poynard, T., The French METAVIR Cooperative Study Group. An algorithm for grading activity in chronic hepatitis C. *Hepatology* **24**, 289–293 (1996).
- Tsai, J. H., Liau, J. Y., Lee, C. H. & Jeng, Y. M. Lymphoepithelioma-like intrahepatic cholangiocarcinoma is a distinct entity with frequent pTERT/TP53 mutations and comprises 2 subgroups based on Epstein-Barr virus Infection. *Am. J. Surg. Pathol.* **45**, 1409–1418 (2021).
- Villanueva, A. Hepatocellular Carcinoma. *N. Engl. J. Med.* **380**, 1450–1462 (2019).
- Schulze, K., Nault, J. C. & Villanueva, A. Genetic profiling of hepatocellular carcinoma using next-generation sequencing. *J. Hepatol.* **65**, 1031–1042 (2016).
- Cancer Genome Atlas Research Network. Comprehensive and integrative genomic characterization of hepatocellular carcinoma. *Cell* **169**, 1327–1341 (2017).
- Totoki, Y. et al. Trans-ancestry mutational landscape of hepatocellular carcinoma genomes. *Nat. Genet.* **46**, 1267–1273 (2014).

- Jiao, Y. et al. Exome sequencing identifies frequent inactivating mutations in BAP1, ARID1A and PBRM1 in intrahepatic cholangiocarcinomas. *Nat. Genet.* **45**, 1470–1473 (2013).
- Sia, D. et al. Massive parallel sequencing uncovers actionable FGFR2-PPHLN1 fusion and ARAF mutations in intrahepatic cholangiocarcinoma. *Nat. Commun.* **6**, 6087 (2015).
- Farshidfar, F. et al. Integrative genomic analysis of cholangiocarcinoma identifies distinct IDH-mutant molecular profiles. *Cell Rep.* **18**, 2780–2794 (2017).
- Hu, B., Lin, J. Z., Yang, X. B. & Sang, X. T. The roles of mutated SWI/SNF complexes in the initiation and development of hepatocellular carcinoma and its regulatory effect on the immune system: a review. *Cell Prolif* **53**, e12791 (2020).
- Masliah-Planchon, J., Bièche, I., Guinebretière, J. M., Bourdeaut, F. & Delattre, O. SWI/SNF chromatin remodeling and human malignancies. *Annu. Rev. Pathol.* **10**, 145–171 (2015).
- Calderaro, J., Ziol, M., Paradis, V. & Zucman-Rossi, J. Molecular and histological correlations in liver cancer. *J. Hepatol.* **71**, 616–630 (2019).
- Calderaro, J. et al. Histological subtypes of hepatocellular carcinoma are related to gene mutations and molecular tumour classification. *J. Hepatol.* **67**, 727–738 (2017).
- Bou-Nader, M. et al. Polyploidy spectrum: a new marker in HCC classification. *Gut* **69**, 355–364 (2020).
- Mittal, P. & Roberts, C. W. M. The SWI/SNF complex in cancer - biology, biomarkers and therapy. *Nat. Rev. Clin. Oncol.* **17**, 435–448 (2020).
- Wilson, B. G. & Roberts, C. W. SWI/SNF nucleosome remodellers and cancer. *Nat. Rev. Cancer* **11**, 481–492 (2011).
- Reisman, D., Glaros, S. & Thompson, E. A. The SWI/SNF complex and cancer. *Oncogene* **28**, 1653–1668 (2009).
- Peña-Llopis, S. et al. BAP1 loss defines a new class of renal cell carcinoma. *Nat. Genet.* **44**, 751–759 (2012).
- Singh, R. R. et al. Intratumoral morphologic and molecular heterogeneity of rhabdoid renal cell carcinoma: challenges for personalized therapy. *Mod. Pathol.* **28**, 1225–1235 (2015).
- Gerber, T. S. et al. SWI/SNF-deficient undifferentiated/rhabdoid carcinoma of the gallbladder carrying a POLE mutation in a 30-year-old woman: a case report. *Diagn. Pathol.* **16**, 52 (2021).
- Chowdhury, B. et al. PBRM1 regulates the expression of genes involved in metabolism and cell adhesion in renal clear cell carcinoma. *PLoS ONE* **11**, e0153718 (2016).
- Porter, E. G. et al. PBRM1 regulates stress response in epithelial cells. *iScience* **15**, 196–210 (2019).
- Rimm, D. L. et al. A prospective, multi-institutional, pathologist-based assessment of 4 immunohistochemistry assays for PD-L1 expression in non-small cell lung cancer. *JAMA Oncol.* **3**, 1051–1058 (2017).
- Teng, F., Meng, X., Kong, L. & Yu, J. Progress and challenges of predictive biomarkers of anti PD-1/PD-L1 immunotherapy: A systematic review. *Cancer Lett.* **414**, 166–173 (2018).
- Mao, T. L., Chu, J. S., Jeng, Y. M., Lai, P. L. & Hsu, H. C. Expression of mutant nuclear beta-catenin correlates with non-invasive hepatocellular carcinoma, absence of portal vein spread, and good prognosis. *J. Pathol.* **193**, 95–101 (2001).
- Ziol, M. et al. Macrotrabecular-massive hepatocellular carcinoma: a distinctive histological subtype with clinical relevance. *Hepatology* **68**, 103–112 (2018).
- Calderaro, J. et al. ESM1 as a marker of macrotrabecular-massive hepatocellular carcinoma. *Clin. Cancer Res.* **25**, 5859–5865 (2019).
- Honeyman, J. N., Simon, E. P., Robine, N., Chiaroni-Clarke, R., Darcy, D. G., Lim, I. I. P. et al. Detection of a recurrent DNAJB1-PRKACA chimeric transcript in fibrolamellar hepatocellular carcinoma. *Science* **343**, 1010–1014 (2014).

#### AUTHOR CONTRIBUTIONS

J.H.T. and Y.M.J. planned the experiments and reviewed the slides; C.H.L. performed the experiments; J.H.T. and J.Y.L. analyzed the data and drafted the paper. All authors read and approved the final paper.

#### FUNDING

This research is supported by grant 110-2320-B-002-021 from the Ministry of Science and Technology, Republic of China.

#### COMPETING INTERESTS

The authors declare no competing interests.

#### ETHICS APPROVAL/CONSENT TO PARTICIPATE

The study was performed under the regulations of the ethics committee of National Taiwan University Hospital and in accordance with the Declaration of Helsinki.

## ADDITIONAL INFORMATION

**Supplementary information** The online version contains supplementary material available at <https://doi.org/10.1038/s41379-021-00970-z>.

**Correspondence** and requests for materials should be addressed to Jau-Yu Liao.

**Reprints and permission information** is available at <http://www.nature.com/reprints>

**Publisher's note** Springer Nature remains neutral with regard to jurisdictional claims in published maps and institutional affiliations.